Molecular Pharmacology Fast Forward. Published on November 3, 2004 as doi:10.1124/mol.104.006205
This article has not been copyedited and formatted. The final version may differ from this version.

MOL6205

Identification of amino acid residues in the insect sodium channel critical for pyrethroid binding

Jianguo Tan*, Zhiqi Liu*, Ruiwu Wang[¶], Zachary Y. Huang, Andrew C. Chen, Michael Gurevitz and Ke Dong[†]

Department of Entomology (J.T., Z.L., R.W., Z.Y.H., K.D.) Ecology, Evolutionary Biology and Behavior Program (Z.Y.H.), and Neuroscience Program (K.D.), Michigan State University. USDA-ARS, Knipling-Bushland U. S. Livestock Insects Research Laboratory (A.C.C.). Department of Plant Sciences, George S. Wise Faculty of Life Sciences, Tel-Aviv University, Israel (M.G.).

[¶]Current address: Departments of Physiology & Biophysics and Biochemistry & Molecular Biology, University of Calgary, Calgary, Albert T2N 4N1, Canada

*These authors contributed equally to this project.

Molecular Pharmacology Fast Forward. Published on November 3, 2004 as DOI: 10.1124/mol.104.006205
This article has not been copyedited and formatted. The final version may differ from this version.

MOL6205

Running title: molecular determinants of the pyrethroid receptor site

Correspondence author:

Ke Dong

Department of Entomology and Neuroscience Program

Michigan State University

East Lansing, MI 48824

Tel: 517-432-2034

Fax: 517-353-5598

Email: dongk@msu.edu

Manuscript information:

31 pages

7 figures

1 table

36 references

238 words in Abstract

887 words in Introduction

763 words in Discussion

Molecular Pharmacology Fast Forward. Published on November 3, 2004 as DOI: 10.1124/mol.104.006205
This article has not been copyedited and formatted. The final version may differ from this version.

Abstract

The voltage-gated sodium channel is the primary target site of pyrethroids, which constitute a major class of insecticides used worldwide. Pyrethroids prolong the opening of sodium channels by inhibiting deactivation and inactivation. Despite numerous attempts to characterize pyrethroid binding to sodium channels in the past several decades, the molecular determinants of the pyrethroid-binding site on the sodium channel remain elusive. Here we show that an F to I substitution at 1519 (F1519I) in segment 6 of domain III (IIIS6) completely abolished the sensitivity of the cockroach sodium channel expressed in *Xenopus* oocytes to all eight structurally diverse pyrethroids examined, including permethrin and deltamethrin. In contrast, substitution by tyrosine (Y) or tryptophan (W) reduced the channel sensitivity to deltamethrin only by 3-10 fold, indicating that an aromatic residue at this position is critical for the interaction of pyrethroids with sodium channels. The F1519I mutation, however, did not alter the action of two other classes of sodium channel toxins, batrachotoxin (a site 2 toxin) and Lqhα-IT (a site 3 toxin). Schild analysis utilizing competitive interaction of pyrethroid stereospecific isomers demonstrated that the F1519W mutation and a previously known pyrethroid-resistance mutation, L993F in IIS6, reduced the binding affinity of 1S cis permethrin, an inactive isomer that shares the same binding site with the active isomer 1R cis permethrin. Our results provide the first direct proof that L993 and F1519 are part of the pyrethroid receptor site on an insect sodium channel.

Molecular Pharmacology Fast Forward. Published on November 3, 2004 as DOI: 10.1124/mol.104.006205
This article has not been copyedited and formatted. The final version may differ from this version.

Introduction

Voltage-gated sodium channels are essential for the initiation and propagation of action potential in the nervous system and other excitable cells (Catterall, 2000). Because of their fundamental role in membrane excitability, sodium channels are an effective target site for a variety of neurotoxins produced by plants and animals for their defense or preying strategies. These sodium channel neurotoxins alter various channel properties, including ion conductance, ion selectivity, activation or inactivation. At least six distinct receptor sites are recognized (Gordon, 1997; Zlotkin 1999; Catterall et al., 2003; Wang and Wang, 2003). Photoaffinity labeling and site-directed mutagenesis approaches have been instrumental in elucidating molecular determinants of these receptor sites (Cestele and Catterall, 2000; Blumenthal and Seibert, 2003). Because of the unique pharmacological effects of various neurotoxins on channel functional properties, studies of toxin binding sites have played an important role in the understanding of sodium channel functions and molecular bases of neurotoxicity.

Pyrethroid insecticides are among the earliest neurotoxins that were identified to act on sodium channels (Narahashi, 2000). They are synthetic analogs of the naturally occurring pyrethrum from the flower extracts of *Chrysanthemum* species. With a few exceptions of more recently developed compounds, pyrethroids are typically esters of chrysanthemic acid (Elliott 1977, also see pyrethroid chemical structures in Fig. 1). The commercial development of synthetic pyrethroids is one of the major success stories in the use of natural products as a source of leads for the production of novel insecticidal compounds. Because of the relatively low mammalian toxicity and favorable environmental properties, pyrethroids represent a major class of insecticides used to control many agriculturally and medically important arthropod pests.

Molecular Pharmacology Fast Forward. Published on November 3, 2004 as DOI: 10.1124/mol.104.006205
This article has not been copyedited and formatted. The final version may differ from this version.

Pyrethroids are classified into type I and type II, based on their chemical structure: type I pyrethroids lack a cyano group at the phenylbenzyl or other alcohols, whereas type II pyrethroids contain an α-cyano-3-phenylbenzyl alcohol. Despite differences in the chemical structure, poisoning syndromes, and their differential effects on the nervous system, both type I and II pyrethroids prolong sodium channel opening by inhibiting inactivation and deactivation, resulting in a slowly decaying tail current associated with repolarization (Narahashi, 2000). Pyrethroids have one to three chiral centers, which may be located at C1 and C3 of the cyclopropane ring and at the αC atom of the alcohol moiety. Type I pyrethroids permethrin and tetramethrin, for example, have four stereospecific isomers: 1R cis, 1R trans, 1S cis, and 1S trans. The stereoisomerism of pyrethroids is critically important for pyrethroid action. 1R cis and 1R trans isomers are active, whereas the other two are not. Furthermore, the inactive 1S cis tetramethrin competes with the active 1R cis tetramethrin for the same binding site and antagonizes the action of the active isomer (Lund and Narahashi, 1982).

The pyrethroid-binding site on the sodium channel has not been defined at the molecular level, and remains a major unresolved issue in sodium channel pharmacology. Substantial evidence from electrophysiological and pharmacological studies indicates that the pyrethroid receptor site is distinct from, yet allosterically coupled with, several other receptor sites, such as site 2 to which batrachotoxin (BTX) binds (Catterall, 1992; Gordon, 1997). Specific binding of radiolabeled pyrethroids was detected in rat brain membrane preparations (Trainer et al., 1997). However, attempts to characterize specific binding of pyrethroids to insect nerve membrane preparations failed because of the extreme

Molecular Pharmacology Fast Forward. Published on November 3, 2004 as DOI: 10.1124/mol.104.006205
This article has not been copyedited and formatted. The final version may differ from this version.

hydrophobicity of pyrethroids resulting in extremely high non-specific binding (Rossignol, 1988; Pauron et al., 1989; Dong, 1993).

Due to intensive use of pyrethroids in arthropod control, many arthropod populations have developed resistance to these compounds. One major mechanism of pyrethroid resistance, known as knockdown resistance (*kdr*), was first discovered in house flies and subsequently in many other insect and arachnid species (Soderlund and Bloomquist, 1990). Extensive research in the past decade convincingly showed that *kdr* and *kdr*-like mechanisms are caused by mutations in sodium channels (Refs, in Dong, 2002; Soderlund and Knipple, 2003). Like mammalian sodium channel α-subunits, the primary structure of insect sodium channel proteins contains four homologous domains (I-IV), each containing six transmembrane segments (S1-S6) (Loughney et al., 1989). To date, more than half a dozen *kdr* mutations have been demonstrated to reduce channel sensitivity to pyrethroids in the *Xenopus* oocyte expression system. An F to I *kdr* mutation in domain III segment 6 (IIIS6), at the position corresponding to F1519 in the cockroach sodium channel, was previously identified in the sodium channel of pyrethroid-resistant southern cattle ticks (*Boophilus microplus*) (He et al., 1999). Substitution of F with I in a recombinant rat $Na_v1.4$ sodium channel reduced the channel sensitivity to a pyrethroid insecticide deltamethrin (Wang et al., 2001).

In this study, we assessed the role of F1519 in pyrethroid binding and action on an insect sodium channel. Our results show that F1519I completely abolished the channel sensitivity to pyrethroids, and that an aromatic residue (F, W or Y) at position 1519 is essential for the action of pyrethroids. By utilizing the competitive binding of active and inactive pyrethroid stereospecific isomers to the sodium channel, we demonstrated that

Molecular Pharmacology Fast Forward. Published on November 3, 2004 as DOI: 10.1124/mol.104.006205
This article has not been copyedited and formatted. The final version may differ from this version.

F1519W reduced the pyrethroid binding to the cockroach sodium channel. We also show that a *kdr* mutation in IIS6 found in many insect sodium channels (corresponding to the L993F mutation in the cockroach sodium channel) also reduced pyrethroid binding. Together, these results for the first time define specific amino acid residues involved in the pyrethroid receptor site on an insect sodium channel.

Materials and methods

Site-directed mutagenesis. A cockroach sodium channel variant, $BgNa_v1$-1 (formerly KD1), was subjected to site-directed mutagenesis to generate recombinant constructs containing the F1519→I1519, →A1519, →R1519, →W1519, or →Y1519 mutation. Briefly, a 1.4-kb *Eco*47III fragment containing F1519 was excised from $BgNa_v1$-1 and cloned into the pAlter 1 vector of the Altered Sites II *in vitro* Mutagenesis System (Promega, Madison, WI). The 1.4-kb mutated *Eco*47III fragment carrying I1519, A1519, R1519, W1519 or Y1519 was cloned back into $BgNa_v1$-1 to generate mutant channels F1519I, F1519A, F1519R, F1519W, and F1519Y.

Expression of $BgNa_v1$-1 sodium Channels in *Xenopus* Oocytes. Ooctye preparation and cRNA injection was performed as described previously (Tan et al., 2002b). For robust expression of the $BgNa_v1$-1 channel, $BgNa_v1$-1 cRNA was co-injected into oocytes with *Drosophila melanogaster* tipE cRNA (2:1 ratio), which enhances the expression of insect sodium channels in oocytes (Feng et al., 1995; Warmke et al., 1997).

Electrophysiological Recording and Analysis. Sodium currents were recorded using standard two-electrode voltage clamping. The borosilicate glass electrodes were filled with

Molecular Pharmacology Fast Forward. Published on November 3, 2004 as DOI: 10.1124/mol.104.006205
This article has not been copyedited and formatted. The final version may differ from this version.

filtered 3M KCl in 0.5% agarose and had a resistance of 0.5 to 1.0 MΩ. The recording solution was ND-96 consisting of: 96 mM NaCl, 2.0 mM KCl, 1.0 mM $MgCl_2$, 1.8 mM $CaCl_2$, and 10 mM HEPES, pH adjusted to 7.5 with NaOH. Stock solutions of BTX (1 mM) and pyerthroids (100 mM) were dissolved in dimethyl sulfoxide. BTX and pyrethroids were generous gifts from John Daly (National Institutes of Health, Bethesda, MD), and Klaus Naumann and Ralf Nauen (Bayer CropScience), respectively. Stock solution of α-scorpion toxin, LqhαIT (100 μM), was dissolved in distilled water containing 10% bovine serum albumin (BSA) in order to prevent adherence of toxin to the vials. Sodium currents were measured using the oocyte clamp instrument OC725C (Warner Instrument Corp., Hamden, CT), Digidata 1200A, and pCLAMP 6 software interface (Axon Instrument, Foster City, CA). All experiments were performed at room temperature (20-22˚C). Capacitive transient and linear leak currents were corrected using P/N subtraction or by subtraction of records obtained in the presence of 20 nM tetrodotoxin (TTX), which completely blocks the $BgNa_v1$-1 sodium channel (Tan et al., 2002a). The maximal peak sodium current was limited to <2.0 μA to achieve better voltage control by adjusting the amount of cRNA and the incubation time after injection. The effects of pyrethroids, BTX, and LqhαIT were measured 10 min after toxin application.

The voltage-dependence of sodium channel conductance (G) was calculated by measuring the peak current at test potentials ranging from -80 mV to +65 mV in 5-mV increments and divided by $(V-V_{rev})$, where V is the test potential and V_{rev} is the reversal potential for sodium ion. Peak conductance values were normalized to the maximal peak conductance (G_{max}) and fitted with a two-state Boltzmann equation of the form $G/G_{max}= [1+ \exp(V-V_{1/2})/k]^{-1}$, in which V is the potential of the voltage pulse, $V_{1/2}$ is the half maximal voltage for activation, and k is the slope factor.

Molecular Pharmacology Fast Forward. Published on November 3, 2004 as DOI: 10.1124/mol.104.006205
This article has not been copyedited and formatted. The final version may differ from this version.

The voltage-dependence of fast inactivation was determined using 200-ms inactivating pre-pulses from a holding potential of -120 mV to 40 mV in 5-mV increments, followed by test pulses to -10 mV for 20 ms. The peak current amplitude during the test depolarization was normalized to the maximum current amplitude, and plotted as a function of the pre-pulse potential. The data were fitted with a two-state Boltzmann equation of the form $I/I_{max} = [1 + (\exp(V-V_{1/2})/k)]^{-1}$, in which I_{max} is the maximal current evoked, V is the potential of the voltage pulse, $V_{1/2}$ is the half maximal voltage for inactivation, and k is the slope factor.

To determine recovery from fast inactivation, sodium channels were inactivated by a 200-ms depolarizing pulse to -10 mV, then repolarized to -120 mV for an interval of variable durations followed by a 20-ms test pulse to -10 mV. The peak current during the test pulse was divided by the peak current during the inactivating pulse and plotted as a function of duration time between the two pulses.

To determine the development of fast inactivation, prepulse potentials ranging from -80 to -20 mV in 10-mV increments of varying durations were applied from the holding potential of -120 mV followed by a test pulse at -10 mV for 20 msec to determine the fraction of current inactivated during the pre-pulse.

To determine the steady-state slow inactivation, oocytes were held at pre-pulse potentials ranging from -120 to +10 mV in 10-mV increments for 50 seconds. A 100-msec recovery pulse to -120 mV and a 20-msec test pulse to -10 mV were given before returning to the holding potential -120 mV. The peak current amplitude during the test depolarization

Molecular Pharmacology Fast Forward. Published on November 3, 2004 as DOI: 10.1124/mol.104.006205
This article has not been copyedited and formatted. The final version may differ from this version.

was normalized to the maximum current amplitude, and plotted as a function of the pre-pulse potential. The data were fitted with a two-state Boltzmann equation of the form $I/I_{max} = [1 + (\exp(V-V_{1/2})/k)]^{-1}$, in which I_{max} is the maximal current evoked, V is the potential of the voltage pulse, $V_{1/2}$ is the half maximal voltage for inactivation, and k is the slope factor.

Measurement of tail currents induced by pyrethroids. The method for application of pyrethroids in the recording system was identical to that described by Tan et al. (2002a). A disposable perfusion system developed by Tatebayashi and Narahashi (1994) was used, which contained a Petri dish placed on an adjustable support stand, a recording chamber built with glue, and Tygon tubing connecting the Petri dish and the recoding chamber. The solution was delivered by hydrostatic force by adjusting the level of the Petri dish relative to the recording chamber. The pyrethroid-induced tail current was recorded during a 100-pulse train of 5-ms depolarization from –120 mV to 0 mV with a 5-ms inter-pulse interval (Vais et al., 2000). The percentage of channels modified by pyrethroids was calculated using the equation $M=\{[I_{tail}/(E_h-E_{Na})]/[I_{Na}/(E_t-E_{Na})]\} \times 100$ (Tatebayashi and Narahashi, 1994), where I_{tail} is the maximal tail current amplitude, E_h is the potential to which the membrane is repolarized, E_{Na} is the reversal potential for sodium current determined from the I-V curve, I_{Na} is the amplitude of the peak current during depolarization before pyrethroid exposure, and E_t is the potential of step depolarization. The concentration–response data were fitted to the Hill equation: $M = M_{max}/\{1 + (K_d/[P])^n\}$, where [P] represents the concentration of pyrethroid and K_d represents the concentration of pyrethroid that produced the half-maximal effect, n represents the Hill coefficient, and the M_{max} is the maximal percentage of sodium channels modified.

Schild analysis. K_d values were determined from the dose-response curves of the active 1R cis isomer on wild-type and mutant sodium channels by measuring the amplitude of 1R

Molecular Pharmacology Fast Forward. Published on November 3, 2004 as DOI: 10.1124/mol.104.006205
This article has not been copyedited and formatted. The final version may differ from this version.

cis isomer-induced tail current and calculating percentage of channel modification as described above. A series of K_d values (denoted as, K_d') of the active 1R cis isomer were determined in the presence of increasing concentrations of the inactive 1S cis isomer. Schild analysis was employed to determine the affinity of the inactive isomer, calculated from the equation: log(Dose Ratio - 1) = $\log K_B$ - log[B], where Dose Ratio=K_d'/K_d, [B] is the molar concentration of the inactive 1S cis isomer, and K_B is the dissociation constant of the inactive 1S cis isomer. - Log(Dose Ratio -1) was plotted as a function of - log[B]. The data were fitted with a linear regression, generating the Schild plot slope and the X intercept, pA_2, which equals to - $\log K_B$.

Results

Tail Currents Induced by Type I and Type II Pyrethroids. The amplitude and decay kinetics of the tail current are commonly used to quantify the effects of pyrethroids (Tatebayashi and Narahashi, 1994; Vais et al., 2000). For type I pyrethroids, such as bioallethrin, a single long (50 ms) depolarization produced a detectable tail current from wild-type $BgNa_v1$-1 channel. However, no tail current was elicited by a type II pyrethroid, deltamethrin, using the same recording protocol. Detection of deltamethrin-induced tail currents requires a 100-pulse train of 5-ms depolarization from –120 mV to 0 mV with a 5-ms inter-pulse interval (Vais et al., 2000; Tan et al., 2002a). For direct comparison, we used the latter protocol in this study to elicit tail currents by both type I and type II pyrethroids (Fig. 1). Tail currents with amplitudes in the μA range were induced in the wild-type $BgNa_v1$-1 channel by 1 μM deltamethrin or 3 μM of the other six pyrethroids. The two type II pyrethroids, cypermethrin and deltamethrin, induced tail currents decay rather slowly with a biphasic decay (τ_1=1.3 ± 0.5 s and τ_2=0.3 ± 0.07 s for deltamethrin), whereas most type I

Molecular Pharmacology Fast Forward. Published on November 3, 2004 as DOI: 10.1124/mol.104.006205
This article has not been copyedited and formatted. The final version may differ from this version.

pyrethroid-induced tail currents returned to the baseline within 1 s, exhibiting a monophasic decay (τ=268.3 $\pm$ 85.4 ms for 1R cis permethrin). These results are consistent with earlier findings that both type I and type II pyrethroids preferably bind to open sodium channels although type I pyrethroids can also bind to closed sodium channels (Vais et al., 2000; 2003).

F1519I Completely Abolishes the Sensitivity of the Cockroach Sodium Channel to Eight Structurally Diverse Pyrethroids. To date, more than half a dozen *kdr* mutations have been demonstrated to reduce the sensitivity of insect sodium channels to pyrethroids in *Xenopus* oocytes. The F to I mutation was identified in pyrethroid-resistant cattle ticks (He et al., 1999). However, the effect of this mutation on the sensitivity of insect sodium channels to pyrethroids has not been examined. Here we examined the sensitivity of wild-type $BgNa_v1$-1 and the F1519I mutant channel to the eight pyrethroids. We found that in contrast to wild-type $BgNa_v1$-1 channel, no tail current was detected in oocytes expressing the F1519I channel when exposed to any of these eight pyrethroids, even at the highest concentrations used (shown in Fig. 1I for deltamethrin). These results indicate that the F1519I mutant channel is completely insensitive to the eight structurally diverse pyrethroids and that the F1519 residue is critical for pyrethroid action.

The F1519I Mutation Disrupts Fast Inactivation and Alters the Voltage-dependence of Activation. To examine whether the F1519I mutation alters the channel gating properties, sodium current was recorded from a 20-ms depolarization to -10 mV from the holding potential of -120 mV for both the wild type and mutant channels. The F1519I mutation did not alter recovery from fast inactivation, closed-state inactivation, or voltage-dependence of slow inactivation (Fig. 2D, E and F). However, while the wild-type sodium channel was completely inactivated at the end of the depolarizing pulse, the F1519I mutant channel

Molecular Pharmacology Fast Forward. Published on November 3, 2004 as DOI: 10.1124/mol.104.006205
This article has not been copyedited and formatted. The final version may differ from this version.

exhibited a noticeable sustained current (Fig. 2A), suggesting that the F1519I change altered fast inactivation. In addition, the F1519I channel activated more slowly than the wild-type channel (Fig. 2A). The F1519I mutation also shifted the voltage-dependence of activation in the depolarizing direction by ca. 8 mV (Fig. 2B and Table 1). Although the voltage of half steady-state inactivation was not affected by F1519I (Fig. 2C and Table 1), the voltage-dependence of inactivation curve showed incomplete inactivation at positive potentials for the mutant channel, consistent with the detection of the sustained current shown in Fig. 2A.

F1519I does not alter the action of BTX or LqhαIT on sodium channel function. Substantial evidence indicates that amino acid residues in the middle portion of multiple S6 segments are critical components of the BTX receptor site (Refs. in Wang and Wang, 2003; Blumenthal and Seibert, 2003). Interestingly, F1519 is only one amino acid residue apart from S1276 in $Na_v1.4$, which is part of the BTX receptor site (Wang et al., 2000). BTX causes persistent activation of sodium channels at the resting membrane potential by blocking sodium channel inactivation and shifting the voltage dependence of channel activation to more negative membrane potentials (Hille, 1992; Catterall, 1988). Previously, Wang et al. (2001) reported that the rat $Na_v1.4$ mutant channel carrying F1278I (equivalent to F1519I) remained sensitive to BTX. To evaluate whether the F1519I mutation alters the action of BTX on an insect sodium channel, we examined the BTX effects on both wild-type and F1519I channels. At 100 nM, BTX inhibited the inactivation and reduced the amplitude of the peak current of both wild-type and mutant channels, as indicated by the sodium current recording traces (Fig. 3A). Furthermore, two voltage-dependent components were evident from the current-voltage relationship (Fig. 3B), with one similar to that of the unmodified channel and the other exhibiting a 40-mV hyperpolarizing shift, which represents the voltage-dependence of the BTX-modified channels. These effects were quite similar to

Molecular Pharmacology Fast Forward. Published on November 3, 2004 as DOI: 10.1124/mol.104.006205
This article has not been copyedited and formatted. The final version may differ from this version.

those observed on rat sodium channels (Catterall, 1988). There was no difference in the effects of BTX on wild-type and mutant channels (Fig. 3A, B, C), suggesting that the F1519I mutation did not alter the action of BTX on the insect sodium channel.

Previously, positive allosteric interactions between α-scorpion toxins and pyrethroids have been reported (such as, Trainer et al., 1997; Vais et al., 2000; Gilles et al., 2003). Furthermore, a *kdr* mutation in IS6 enhanced the sensitivity of tobacco budworm sodium channels to LqhαIT, an α-scorpion toxin acting on site 3 (Lee et al., 1999). LqhαIT shifts the voltage-dependence of activation of sodium channels in the depolarizing direction in house fly neurons (Lee et al., 2000). We examined the effect of F1519I on the action of LqhαIT. At 10 nM, LqhαIT nearly abolished channel inactivation during a 20-ms depolarization to -10 mV after 10 min pre-incubation with the toxin (Fig. 4A, C). This toxin also increased the amplitude of peak current by 2-fold (Fig. 4A). These effects are typical of site 3 sodium channel toxins (Lee et al., 1999; Lee and Adams, 2000; Vais et al., 2000). LqhαIT produced a similar degree of modification in the F1519I mutant channel (Fig. 4A, right panel), indicating the F1519I did not alter the channel sensitivity to LqhαIT. Furthermore, consistent with what was observed in house fly neurons after application of LqhαIT (Lee et al., 2000), LqhαIT shifted the voltage-dependence of activation by 10 mV in the depolarizing direction for both wild-type and mutant channels (Fig. 4B). LqhαIT also increased the amplitudes of deltamethrin- and bioallethrin-induced tail currents in the wild-type channel by 5-fold (Fig 4D, E). This enhancement likely results from an increasing in the availability of open channels as the result of eliminating channel inactivation and increasing the peak current (Vais et al., 2000). However, even in the presence of the LqhαIT-mediated enhancement, no tail current was detected in the F1519I channel. Thus, F1519I appears to be unique among all

Molecular Pharmacology Fast Forward. Published on November 3, 2004 as DOI: 10.1124/mol.104.006205
This article has not been copyedited and formatted. The final version may differ from this version.

examined *kdr* mutations in that it alone is sufficient to completely block pyrethroid action on an insect sodium channel.

An Aromatic Amino Acid Residue at Position 1519 is Required for the Action of Pyrethroids. To determine how critical the amino acid side chain at 1519 position is for the action of pyrethroids, we made four additional amino acid substitutions at 1519: alanine (A, hydrophobic), arginine (R, positively charged), tryptophan (W, aromatic), and tyrosine (Y, aromatic). The F1519R channel did not produce any detectable sodium current in oocytes, whereas the peak currents of other three mutant channels were comparable to that of the wild-type $BgNa_v1$-1 channel. Like the F1519I mutant channel, these three mutant channels shifted the voltage-dependence of activation in the depolarizing direction, with the largest shift of 13-mV for the F1519W channel (Fig. 5A and Table1). None of the substitutions altered the voltage-dependence of inactivation (Fig. 3B and Table 1). Unlike the F1519I mutant channel, the other three mutant channels completely inactivated at positive membrane potentials without generating a non-inactivating current (data not shown).

We next examined the effect of the A, W, and Y amino acid substitutions on the pyrethroid-induced tail current. The aromatic residue substitutions Y and W only slightly reduced the amplitude of tail current induced by 1 μM deltamethrin, compared with that induced in the wild-type channel (Fig. 5C). The EC_{20} was 0.2, 0.7, and 2.2 μM for the wild-type, F1519Y, and F1519W channels, respectively (Fig. 5D), resulting in a reduction of 3 to 11 fold in their sensitivity to deltamethrin. However, the tail current was not detectable for the F1519A channel at 1 μM deltamethrin and only a small tail current was detected at 100 μM deltamethrin (Fig. 5C). These results demonstrated that an aromatic residue at position 1519 in IIIS6 is required for deltamethrin action.

Molecular Pharmacology Fast Forward. Published on November 3, 2004 as DOI: 10.1124/mol.104.006205
This article has not been copyedited and formatted. The final version may differ from this version.

The F1519W Mutation Reduces the Binding of 1S cis Permethrin to BgNa$_v$ channel. In all previous studies by us and others, the effects of *kdr* mutations on pyrethroid binding and action were assessed by quantifying the modification of sodium channels by pyrethroids and fitting the data to the Hill equation: $M = M_{max}/\{1+(K_d/[P])^n\}$. Increases in K_d or EC_{50} values for *kdr* mutant channels reflect reduced sensitivities of these mutant channels to pyrethroids. However, an increase in K_d or EC_{50} does not necessarily represent a reduction in pyrethroid binding to the sodium channel. K_d is an apparent dissociation constant; a change in the K_d value could be the result of i) a direct alteration of the binding site, and/or ii) a non-binding-site alteration that allosterically uncouples pyrethroid binding from subsequent sodium channel modification. Therefore, whether or not the effect of a *kdr* mutation on sodium channel sensitivity to pyrethroids results from a direct alteration of the pyrethroid binding site has never been determined in all previous studies. In this study, we took advantage of the competitive binding of active and inactive pyrethroid isomers to the sodium channel to directly evaluate the pyrethroid binding affinity of the inactive isomer using the Schild analysis.

Consistent with the finding by Lund and Narahashi (1982), we found that the inactive 1S cis permethrin decreased the amplitude of the tail current induced by the active 1R cis permethrin, but did not induce any tail current by itself (Fig. 6A). We then determined the percentage of channel modification by the active 1R cis isomer in the presence of increasing concentrations of the inactive 1S cis isomer. The presence of the inactive 1S cis isomer shifted the dose-response curve for the active isomer to the right (Fig. 6B, C and D), confirming that 1S cis isomer is an antagonist of the active 1R cis isomer on the cockroach sodium channel.

Molecular Pharmacology Fast Forward. Published on November 3, 2004 as DOI: 10.1124/mol.104.006205
This article has not been copyedited and formatted. The final version may differ from this version.

The F1519I mutant channel is completely insensitive to pyrethroids and is thus not useful for binding affinity analysis. We therefore conducted the Schild analysis using the F1519W channel that exhibits an intermediate sensitivity to deltamethrin. Schild analysis (Fig. 6B, C and D) showed a linear regression with a slope of 0.84 and 0.62 for wild-type and F1519W channels, respectively. The X intercept pA_2, which equals to -log K_B (the dissociation constant of the inactive 1S cis isomer), was 6.0 for the wild-type channel and 4.3 for the F1519W channel (Fig. 6E), corresponding to a K_B of 1.2 μM for the wild-type channel and a K_B of 53 μM for the F1519W mutant channel. Therefore, the F1519W mutation caused a 45-fold reduction in the binding affinity of 1S cis permethrin to the cockroach sodium channel, indicating that F1519 is part of the pyrethroid binding site.

The L993F *kdr* Mutation Also Reduces the Binding of 1S cis Permethrin to $BgNa_v$. A *kdr* mutation (corresponding to L993F in the cockroach sodium channel) found in many insect species reduces the pyrethroid sensitivity of the cockroach sodium channel by 5-fold (Tan et al., 2002a). We examined the binding affinity of the inactive 1S cis permethrin isomer for the L993F channel using the Schild analysis. Our analysis showed that the X intercept pA_2 (i.e., - log K_B) was 4.8, corresponding to a K_B of 16 μM for this mutant channel (Fig. 6D and 6E). Therefore, L993F reduced the binding affinity of the inactive isomer by 16-fold, compared to the wild-type channel. This result demonstrates that L993 is also part of the pyrethroid receptor site.

Discussion

As an important class of insecticides that target sodium channels, pyrethroids have attracted much attention in the study of the pharmacological and electrophysiological

Molecular Pharmacology Fast Forward. Published on November 3, 2004 as DOI: 10.1124/mol.104.006205
This article has not been copyedited and formatted. The final version may differ from this version.

aspects of sodium channels in the past several decades. However, the pyrethroid-binding site on the sodium channel has eluded molecular characterization despite serious efforts to understand it. Even though specific binding of pyrethroids to rat brain membrane preparations has been reported (Trainer et al., 1997), many attempts to measure specific pyrethroid binding in insect nerve tissue preparations using similar methods were unsuccessful. The recent identification of a series of *kdr* sodium channel mutations that confer pyrethroid resistance on insects brought us closer to the understanding of this site, because some *kdr* mutations are expected to affect pyrethroid binding. However, a direct demonstration of the effect of a *kdr* mutation on pyrethroid binding is lacking. In this study, we show that 1) an F1519I mutation in IIIS6 completely abolished the sensitivity of the cockroach sodium channel to diverse type I and type II pyrethoids; 2) this mutation alters the channel gating properties, but does not affect the action of site 2 (BTX) or site 3 (LqhαIT) sodium channel toxins; 3) an aromatic residue at position 1519 is required for the action of pyrethroids; and 4) mutations F1519W and L993F reduced the binding affinity of pyrethroids to the cockroach sodium channel. Our work therefore provides direct evidence for the involvement of F1519 in IIIS6 and L993 in IIS6 in forming the elusive pyrethroid-binding site.

Our amino acid substitution experiments suggest that an aromatic residue at position 1519 of the cockroach sodium channel is essential for pyrethroid binding. More than a decade ago, Klaus Naumann proposed a “horseshoe model” for pyrethroid action, based on pyrethroid structure-activity relations, stereochemical information, and toxicity data (Naumann, 1990). This model predicted that the binding site (pocket) for active pyrethroids, in which the pyrethroid curves into a horseshoe shape, is possibly at an aromatic residue of the sodium channel backbone, and suggested a common active conformation for the structurally diverse pyrethroids at the sodium channel. Our findings presented in this paper

Molecular Pharmacology Fast Forward. Published on November 3, 2004 as DOI: 10.1124/mol.104.006205
This article has not been copyedited and formatted. The final version may differ from this version.

support this long-standing model and suggest that F1519 is probably the aromatic residue in Naumann's horseshoe model.

Substitutions of the leucine residue in IIS6 (corresponding to L993 in $BgNa_v$) have been found in diverse insect species and appear to be the most common type of naturally occurring *kdr* mutations in insects (Dong, 2002; Soderlund and Knipple, 2003). We showed that the L993F mutation, like F1519I mutation, reduced pyrethroid binding to the cockroach sodium channel. Thus, it seems that natural selection also favored residues in the pyrethroid-binding site to reduce pyrethroid action.

It has been suggested from previous electrophysiological studies using nerve preparations or sodium channels expressed in oocytes that pyrethroids interact with the sodium channel at multiple sites (Lund and Narahashi, 1982; Vais et al., 2002; 2003). For example, it was suggested that the super-*kdr* mutation M918T in the loop connecting IIS4-S5 of the house fly sodium channel eliminates one of the pyrethroid action sites (Vais, 2000; 2003). We show here that the F1519I mutation completely abolishes sodium channel sensitivity to structurally diverse pyrethroids. If the multiple binding site theory is correct, binding at F1519 must be a prerequisite for pyrethroid binding and action on other sites. A lack of the initial binding of pyrethroids to F1519 may prevent subsequent pyrethroid interactions with other residues, such as L993 and M918. An initial binding at F1519 could induce conformational changes necessary for the formation of an optimal pyrethroid binding site. Both F1519 and L993 are located in the 6th transmembrane. However, other *kdr* or *kdr*-like mutations in different arthropods are not confined in S6 segments. Several mutations are found in the intracellular linkers or loops close to the transmembrane segments. In the folded sodium channel many of these residues could be localized in close proximity. Therefore, conformational transitions induced by an initial pyrethroid binding to

Molecular Pharmacology Fast Forward. Published on November 3, 2004 as DOI: 10.1124/mol.104.006205
This article has not been copyedited and formatted. The final version may differ from this version.

F1519 may reorient some of these neighboring residues to form optimal pyrethroid-binding site(s) in the intracellular side of the channel. Interestingly, a similar multi-step binding model has been proposed for the interaction between epinephrine and its receptor, β_2 adrenergic receptor (Kobilka 2004, Liapakis et al., 2004).

In summary, we show here that two residues defined by *kdr* mutations in the 6th transmembrane segments of the cockroach sodium channel are part of the long-sought-after pyrethroid-binding site. Further examination of the role(s) of other *kdr* or *kdr*-type mutations in pyrethroid binding and action should lead to a better understanding of the molecular details of the pyrethroid receptor site on the sodium channel.

Acknowledgements

We thank Drs. Klaus Naumann and Ralf Nauen (Bayer CropScience), and John Daly (National Institutes of Health) for the generous gift of permethrin isomers and other pyrethroids, and BTX, respectively. We also thank Drs. Dalia Gordon and Noah Koller for critical review of this manuscript.

Molecular Pharmacology Fast Forward. Published on November 3, 2004 as DOI: 10.1124/mol.104.006205
This article has not been copyedited and formatted. The final version may differ from this version.

References

Blumenthal KM and Seibert AL (2003) Voltage-gated sodium channel toxins: poisons, probes, and future promise. *Cell Biochem Biophys*. **38:**215-238.

Catterall WA (1988) Molecular pharmacology of voltage-sensitive sodium channels*. ISI Atlas Sci. Pharmacol.* 190-195.

Catterall W A (1992) Cellular and molecular biology of voltage-gated sodium channels. *Physiol. Rev.* **72**: S15-48.

Catterall WA (2000) From ionic currents to molecular mechanisms: the structure and function of voltage-gated sodium channels. *Neuron* **26**:13-25.

Catterall WA, Goldin AL, and Waxman SG (2003) International Union of Pharmacology. XXXIX. Compendium of voltage-gated ion channels: sodium channels. *Pharmacol Rev* **55**:575-578.

Cestele S and Catterall WA (2000) Molecular mechanisms of neurotoxin action on voltage-gated sodium channels. *Biochimie* **82**:883-892.

Dong K (1993) Molecular characterization of knockdown (*kdr*)-type resistance to pyrethroid insecticides in the German cockroach (*Blattella germanica* L.). Ph.D. Dissertation, Cornell University.

Dong K (2002) Voltage-gated sodium channels as insecticide targets. In *Chemistry of Crop Protection: Progress and Prospects in Science and Regulation*, (Voss G. and Ramos G. eds) pp.167-176.

Elliott M (1977) Synthetic pyrethroids. In *Synthetic Pyrethroids*, Elliott M ed) pp1-27, American Chemical Society, Washington DC.

Feng G, Deak P, Chopra M, and Hall LM (1995) Cloning and functional analysis of TipE, a novel membrane protein that enhances *Drosophila* Para sodium channel function. *Cell* **82:** 1001-1011.

Gilles N, Gurevitz M, and Gordon D (2003) Allosteric interactions among pyrethroid, brevetoxin, and scorpion toxin receptors on insect sodium channels raise an alternative approach for insect control. *FEBS Letters* **540:** 81-85.

Gordon D (1997) Sodum channels as targets for neurotoxins: mode of action and interaction of neurotoxins with receptor sites on sodium channels. in: *Toxins and Signal Transduction* (Lazarovici P and Gutman Y eds.) pp. 119–149, Harwood Academic Publishers, Amsterdam, the Netherlands.

He H, Chen AC, Davey RB, Ivie GW, and George JE (1999) Identification of a point mutation in the *para*-type sodium channel gene from a pyrethroid-resistant cattle tick. *Biochem. Biophys. Res Comm* **261:** 558-561.

Hille B (1992) *Ionic channels of excitable membranes* (Hille B ed) Sinauer Associates, Inc. Sunderland, Massachusetts.

Kobilka B (2004) Agonist binding: A multistep process. *Mol Pharmacol* **65:**1060-1062.

Lee D, Gurevitz M, and Adams ME (2000) Modification of synaptic transmission and sodium channel inactivation by the insect-selective scorpion toxin LqhαIT. J. Neurophysiol. **83**:1181-1187.

Liapakis G, Chan WC, Papadokostaki M, and Javitch JA (2004) Synergistic contributions of the functional groups of epinephrine to its affinity and efficacy at the β_2 adrenergic receptor. *Mol Pharmacol* **65:**1181-1190.

Loughney K, Kreber R and Ganetzky B (1989) Molecular analysis of the *para* locus, a sodium channel gene in *Drosophila*. *Cell* **58**: 1143–1154.

Lund AE and Narahashi T (1982) Dose-dependent interaction of the pyrethroid isomers with sodium channels of squid axon membranes. *NeuroTox* **3:** 11-24.

Narahashi T (2000) Neuroreceptors and ion channels as the basis for drug action: past, present, and future. *J Pharmacol Exp Ther* **294:**1-26.

Naumann K (1990) Synthetic pyrethroid insecticides: structures and properties in: *Chemistry of Plant Protection: Synthetic Pyrethroid Insecticides* (Huang G and Hoffmann, eds.) pp ----, Springer-Verlag.

Pauron D, Barhanin J, Amichot M, Pralavorio M, Berge J-B, and Lazdunski M (1989) Pyrethroid receptor in the insect Na^+ channel: alteration of its properties in pyrethroid-resistant flies. *Biochemistry* **28:** 1673-1677.

Rossignol DP (1988) Reduction in number of nerve membrane sodium channels in pyrethroid resistance house flies. *Pestic Biochem Physiol* **32:**146-152.

Soderlund DM and Bloomquist JR (1990) Molecular mechanisms of insecticide resistance, in *Pesticide Resistance in Arthropods* (Roush RT and Tabashnik BE eds.) pp. 58-96, Chapman and Hall, New York.

Soderlund DM and Knipple DC (2003) The molecular biology of knockdown resistance to pyrethroid insecticides. *Insect Biochem Molec Biol* **33:**563-577.

Tan J, Liu Z, Tsai T, Valles SM, Goldin AL, and Dong K (2002a) Novel sodium channel gene mutations in *Blattella germanica* reduce the sensitivity of expressed channels to deltamethrin. *Insect Biochem Molec Biol* **32:**445-454.

Tan J, Liu Z, Nomura Y, Goldin AL, and Dong K (2002b) Alternative splicing of an insect sodium channel gene generates pharmacologically distinct sodium channels. *J Neurosci* **22:** 5300-5309.

Tatebayashi H and Narahashi T (1994) Differential mechanism of action of the pyrethroid tetramethrin on tetrodotoxin-sensitive and tetrodotoxin-resistant sodium channels. *J Pharmacol Exp Ther* **270:** 595-603.

Trainer VL, McPhee JC, Boutelet-Bochan H, Baker C, Scheuer T, Babin D, Demoute JP, Guedin D, and Catterall WA (1997) High affinity binding of pyrethroids to the α-subunit of brain sodium channel. *Mol Pharmacol* **51:** 651-657.

Vais H, Williamson MS, Goodson SJ, Devonshire AL, Warmke JW, Usherwood PNR, and Cohen C (2000) Activation of *Drosophila* sodium channels promotes modification by deltamethrin: reductions in affinity caused by knock-down resistance mutations. *J Gen Physiol* **115:** 305-318.

Vais H, Atkinson S, Pluteanu F, Goodson SJ, Devonshire AL, Williamson MS, and Usherwood PNR (2003) Mutations of the *para* sodium channel of *Drosophila melanogaster* identify putative binding sites for pyrethroids. *Mol Pharmacol* **64:**914-922.

Wang SY, Barile M, and Wang GK (2001) A phenylalanine residue at segment D3-S6 in Nav1.4 voltage-gated Na^+ channels is critical for pyrethroid action. *Mol Pharmacol* **60:**620-628.

Wang SY, Nau C, and Wang GK (2000) Residues in Na^+ channel D3-S6 segment modulate both batrachotoxin and local anesthetic affinities. *Biophys J* **79**:1379-1387.

Wang SY and Wang GK (2003) Voltage-gated sodium channels as primary targets of diverse lipid-soluble neurotoxins. *Cell Signal* **15:**151-159.

Warmke JW, Reenan RAG, Wang P, Qian S, Arena JP, Wang J, Wunderler D,

Liu K, Kaczorowski GJ, Van Der Ploeg LHT, Ganetzky B and Cohen CJ (1997) Functional expression of *Drosophila para* sodium channels: Modulation by the membrane protein tipE and toxin Pharmacology. *J Gen. Physiol.* **110:**119-133.

Zlotkin E. (1999) The insect voltage-gated sodium channel as target of insecticides. *Annu. Rev. Entomol.* **44:** 429-455.

Molecular Pharmacology Fast Forward. Published on November 3, 2004 as DOI: 10.1124/mol.104.006205
This article has not been copyedited and formatted. The final version may differ from this version.

Footnotes:

The study was supported by an NIH grant (GM057440) to K.D., a GREEEN grant (GR99-037) from Michigan State University to K.D. and Z.Y.H., and a BARD grant (IS-3480-03) to K.D. and M.G.

Molecular Pharmacology Fast Forward. Published on November 3, 2004 as DOI: 10.1124/mol.104.006205
This article has not been copyedited and formatted. The final version may differ from this version.

Figure legends

Figure 1. Tail currents induced by bioallethrin, bioresmethrin, tetramethrin, permethrin, NAK5710, fenfluthrin, cypermethrin, and deltamethrin in $BgNa_v1$-1 wild-type channel (A-H),. No tail current was induced in the F1519I mutant channel even at 100 μM deltamethrin (I). The chemical structure of the pyrethroids tested is shown in each inset. The tail current was elicited by 100-pulse of a 67-Hz train of 5-ms depolarization from –120 mV to 0 mV. The tail current decay was best fitted with one exponential with the time constant of 268.3 ± 85.4 ms for 1R cis permethrin, and two exponentials with time constants τ_1=1.3 ± 0.5 s and τ_2=0.3 ± 0.07 s for deltamethrin.

Figure 2. The F1519I mutation affects sodium channel activation and inactivation. A, Sodium current measured from a 20 ms test pulse at –10 mV testing potential from a holding potential of –120 mV in $BgNa_v1$-1 wild-type and F1519I mutant channels. B, Voltage-dependence of activation. The voltage-dependence of sodium channel activation (G) was calculated from the equation $G_{Na} = I_{Na}/(V - V_{rev})$, where I_{Na} is the peak current elicited at the test potential ranging from –80 mV to +65 mV in 5 mV increments, V is the test potential, and V_{rev} is the reversal potential of the sodium current. Peak conductance values were normalized with respect to the maximal peak conductance (G_{max}) and fitted to a two-state Boltzmann equation $G/G_{max} = [1 + \exp(V - V_{1/2})/k]^{-1}$, where V is the potential amplitude of test pulse, $V_{1/2}$ is the half maximal voltage for activation, and k is the slope factor. The average of the half maximal voltage for activation ($V_{1/2}$) and slope factor (k) for $BgNa_v1$-1 wild-type and mutant channels are shown in Table 1. The normalized peak conductance was plotted against the potential of test pulses. C, Recovery from fast inactivation for wild-type and F1519I mutant channels. The recovery rate from fast inactivation was measured

Molecular Pharmacology Fast Forward. Published on November 3, 2004 as DOI: 10.1124/mol.104.006205
This article has not been copyedited and formatted. The final version may differ from this version.

using a two-pulse protocol, in which channels were fast inactivated by a 200 ms voltage pulse of –10 mV, then they were allowed to recover at –120 mV for an increasing time, and finally a 20 ms of –10 mV test pulse was applied to test for the fraction of the channels recovered. Peak currents obtained during the test pulse were normalized to the peak current obtained during the inactivated pulse. The normalized peak currents were plotted versus recovery time. D, Voltage-dependence of steady-state inactivation for wild-type and F1519I mutant channels. The voltage-dependence of fast inactivation was determined using 200 ms pre-pulse potentials ranging from –120 mV to 40m V in 5 mV increments, and then a –10 mV test pulse for 20-ms. Peak currents obtained during the test pulse were normalized with respect to the maximal peak current (I_{max}) and fitted to a two-state Boltzmann equation $I/I_{max} = [1 + \exp(V - V_{1/2})/k]^{-1}$, where V is the potential amplitude of test pulse, $V_{1/2}$ is the half maximal voltage for inactivation, and k is the slope factor. The average of the half maximal voltage for activation ($V_{1/2}$) and slope factor (k) for $BgNa_v1$-1 wild-type and mutant channels are shown in Table 1. The normalized peak current was plotted as a function of the pre-pulse potential. E, Development of fast inactivation. The development of fast inactivation was determined by applying pre-pulse potentials ranging from –80 mV to –20 mV in 10 mV increments of varying duration from a holding potential of –120 mV and then applying a test pulse of –10 mV for 20-ms to measure the fraction of sodium current inactivated during the pre-pulse. Data for development of inactivation (open symbols) and recovery from fast inactivation (filled symbols) were fitted to a single-exponential function and plotted as a function of the development-recovery pulse voltage. The average time constants from wild-type channel (squares, n = 5) and F1519I mutant channel (triangles, n = 4) are shown. F, Voltage-dependence of slow inactivation. Oocytes were held at pre-pulse potentials ranging from –120 mV to +10 mV in 10 mV increments for 50-sec. A 100-ms recovery pulse to –120 mV and then a 20-ms test pulse to –10 mV were given before returning to the holding potential of –120 mV. Peak currents obtained during the test pulse were normalized with

Molecular Pharmacology Fast Forward. Published on November 3, 2004 as DOI: 10.1124/mol.104.006205
This article has not been copyedited and formatted. The final version may differ from this version.

respect to the maximal peak current (I_{max}) and plotted as a function of the pre-pulse potential. The data were fitted to a two-state Boltzmann equation $I/I_{max} = [1 + \exp(V - V_{1/2})/k]^{-1}$, where V is the potential amplitude of test pulse, $V_{1/2}$ is the half maximal voltage for inactivation, and k is the slope factor.

Figure 3. Effects of BTX on the functional properties of wild-type (left panel) and F1519I mutant (right panel) channels. A, Sodium current traces elicited by a 20 ms test pulse to –10 mV from a holding potential of –120 mV before and after the application of 100-nM BTX. With 100-nM BTX in recording chamber, a series of 3000 pulses to –10 mV for 10 ms was applied at 10Hz, and then the sodium current was recorded (traces labeled BTX 100 nM). B, The voltage-dependence of activation curves and C, steady-state inactivation curves generated before and after 100 nM BTX modification. Activation and inactivation curves were determined as described in the legend of Fig 2 (B and D).

Figure 4. Effects of the scorpion toxin, LqhαIT, on the functional properties of wild-type (left panels) and F1519I mutant (right panels) channels. A, Sodium current traces elicited by a 20 ms test pulse to –10 mV from a holding potential of –120 mV before and after the application of 10 nM LqhαIT. B and C, LqhαIT altered the voltage-dependence of activation (B) and steady-state inactivation (C) of the wild-type and F1519I mutant channels. Activation and inactivation curves were determined as described in the legend of Fig 2 (B and D). D and E, LqhαIT enhanced the amplitude of tail current induced by deltamethrin (D) and bioallethrin (E) in wild-type channels (left panels), not in F1519I mutant channels (right panels). The tail current was elicited by 100-pulses of a 67Hz train of 5 ms depolarization from –120 mV to 0 mV.

Molecular Pharmacology Fast Forward. Published on November 3, 2004 as DOI: 10.1124/mol.104.006205
This article has not been copyedited and formatted. The final version may differ from this version.

Figure 5. Amino acid substitutions at F1519 alter sodium channel gating and sensitivity to deltamethrin. A, Voltage-dependence of activation. B, Voltage-dependence of steady-state inactivation. Activation and inactivation curves were determined as described in the legend of Fig 2 (B and D). The average of the half maximal voltage for activation ($V_{1/2}$) and slope factor (k) for $BgNa_v1$-1 wild-type and mutant channels are shown in Table 1. C, Tail currents induced by deltamethrin. The tail current was elicited during a 100-pulse train of 5ms depolarization from –120 mV to 0 mV with a 5ms inter-pulse interval. The tail current decay was best fitted with two exponentials with the time constants τ_1=1.5 ± 0.3 s and τ_2=0.3 ± 0.03s for the F1519Y channel; τ_1=0.9 ± 0.4 s and τ_2=0.3 ± 0.03 s for the F1519W channel. However, the decay of the tail current in the F1519A channel was best fitted with one exponential with the time constant of τ=103.9 ± 47.7 ms. D, Percentage of channel modification by deltamethrin. The percentage of channels modified by pyrethroids was calculated using the equation $M=\{[I_{tail}/(E_h-E_{Na})]/[I_{Na}/(E_t-E_{Na})]\} \times 100$ (Tatebayashi and Narahashi, 1994), where I_{tail} is the maximal tail current amplitude, E_h is the potential to which the membrane is repolarized, E_{Na} is the reversal potential for sodium current determined from the I-V curve, I_{Na} is the amplitude of the peak current during depolarization before pyrethroid exposure, and E_t is the potential of step depolarization. The concentration–response data were fitted to the Hill equation: $M = M_{max}/\{1 + (K_d/[P])^n\}$, where [P] represents the concentration of pyrethroid and K_d represents the concentration of pyrethroid that produced the half-maximal effect, n represents the Hill coefficient, and the M_{max} is the maximal percentage of sodium channels modified.

Figure 6. The F993L and F1519W mutations reduce the binding of 1S cis permethrin to the cockroach sodium channel. A, Inactive 1S cis permethrin antagonizes the action of 1R cis permethrin. No tail current was induced by 1S cis permethrin alone. Tail currents induced

Molecular Pharmacology Fast Forward. Published on November 3, 2004 as DOI: 10.1124/mol.104.006205
This article has not been copyedited and formatted. The final version may differ from this version.

by 1R cis permethrin were reduced with co-application of 1S cis permethrin. Tail currents induced by 1 μM 1R cis permethrin in the absence and presence of the inactive 1 μM 1S cis permethrin are shown. B, C, and D, Channel modification by 1R cis permethrin in the presence of a series of concentrations of 1S cis permethrin in wild-type (B), F1519W (C) and L993F (D) channels. The percentage of channels modified by pyrethroids was calculated as described in the legend of Fig 5 (D). The modification curves were linearized by a logarithm of modification percentage at the Y-axis to estimate accurately the EC_{20} value of each line. E, Schild plots (i.e., pA_2 plots) showing the reduced binding affinity of 1S cis permethrin to the L993F and F1519W channels compared with the wild-type channel. Each datum point represents the average of four oocytes. K_d values were determined from the dose-response curves of the active 1R cis isomer on wild-type, F1519W and L993F mutant sodium channels by measuring the amplitude tail current induced by 1R cis permethrin and calculating percentage of channel modification as described above. A series of K_d values (denoted as, K_d') of the active 1R cis isomer were determined in the presence of increasing concentrations of the inactive 1S cis isomer. Schild analysis was employed to determine the affinity of the inactive isomer, calculated from the equation: $\log(\text{Dose Ratio} - 1) = \log K_B - \log[B]$, where Dose Ratio=$K_d'/K_d$, [B] is the molar concentration of the inactive 1S cis isomer, and K_B is the dissociation constant of the inactive 1S cis isomer. -Log(Dose Ratio - 1) was plotted as a function of -Log[B]. The data were fitted with a linear regression, generating the Schild plot slope and the X intercept, pA_2, which equals to $-\log K_B$.

Figure 7. A schematic diagram of cockroach BgNav sodium channel topology. Four homologous domains (I, II, III, and IV), each containing six transmembrane segments (S1-S6), are indicated. The L993F and F1519I mutations are located in IIS6 and IIIS6, respectively.

Molecular Pharmacology Fast Forward. Published on November 3, 2004 as DOI: 10.1124/mol.104.006205
This article has not been copyedited and formatted. The final version may differ from this version.

Table 1 Voltage dependence of activation and inactivation of Wild-type and mutant sodium channels

Na^+ Channel	Mutations	Activation		Inactivation	
		$V_{1/2}$ (mV)	K (mV)	$V_{1/2}$ (mV)	K (mV)
Wild-type	Wild-type	-23.9 ± 0.2	5.5 ± 0.2	-43.6 ± 1.2	5.3 ± 0.3
I	F1519I	-16.1 ± 0.8	7.5 ± 0.7	-43.5 ± 1.2	6.7 ± 0.5
A	F1519A	-16.2 ± 1.8	7.4 ± 1.4	-42.8 ± 1.6	5.6 ± 0.1
W	F1519W	-10.7 ± 2.4	7.9 ± 0.7	-42.5 ± 1.5	6.4 ± 0.2
Y	F1519Y	-19.4 ± 1.1	6.7 ± 0.6	-43.1 ± 0.9	5.8 ± 0.2

Figure 1

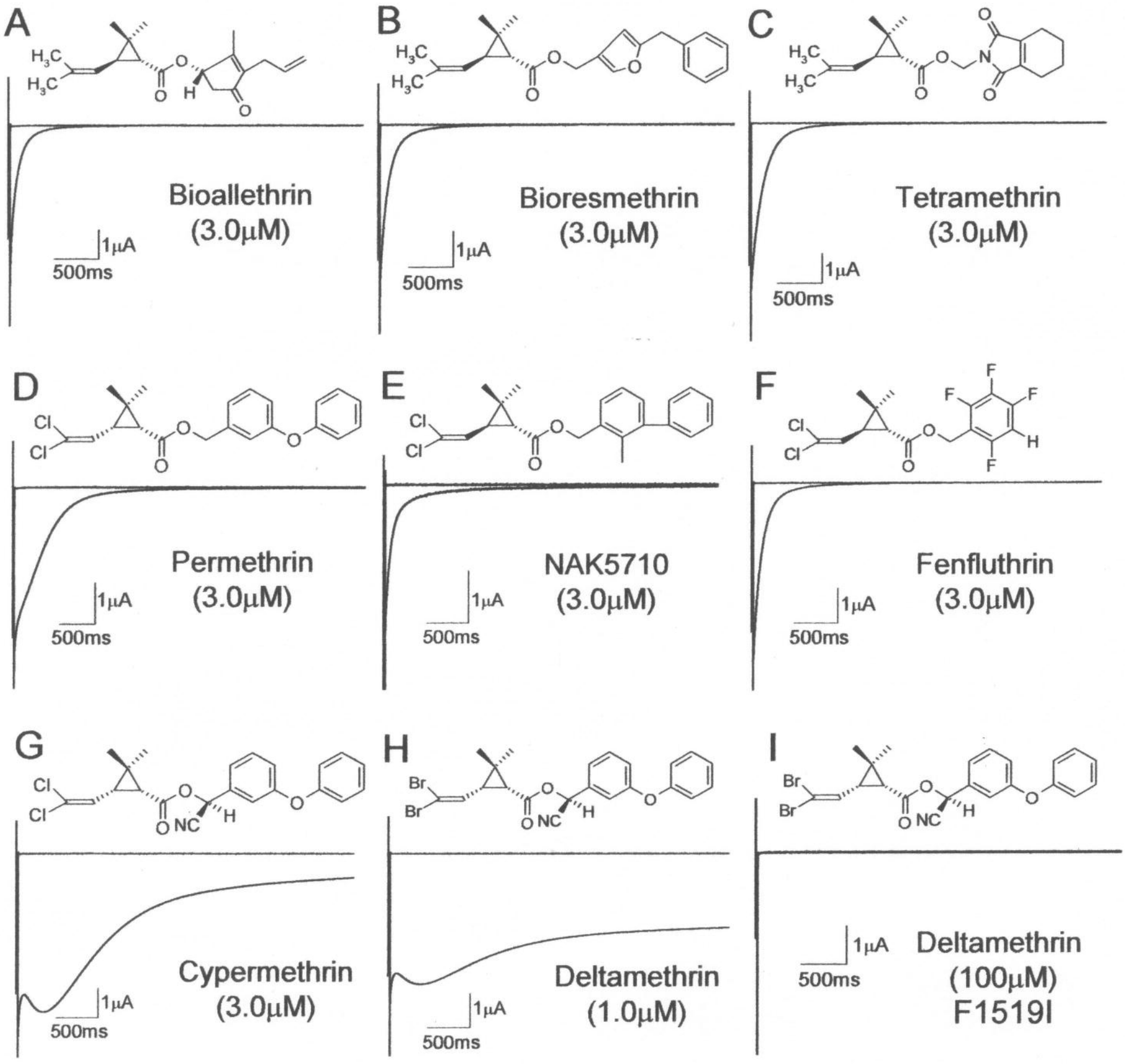
A
Bioallethrin
(3.0μM)
1μA
500ms
B
Bioresmethrin
(3.0μM)
1μA
500ms
C
Tetramethrin
(3.0μM)
1μA
500ms
D
Permethrin
(3.0μM)
1μA
500ms
E
NAK5710
(3.0μM)
1μA
500ms
F
Fenfluthrin
(3.0μM)
1μA
500ms
G
Cypermethrin
(3.0μM)
1μA
500ms
H
Deltamethrin
(1.0μM)
1μA
500ms
I
Deltamethrin
(100μM)
F1519I
1μA
500ms

Figure 2

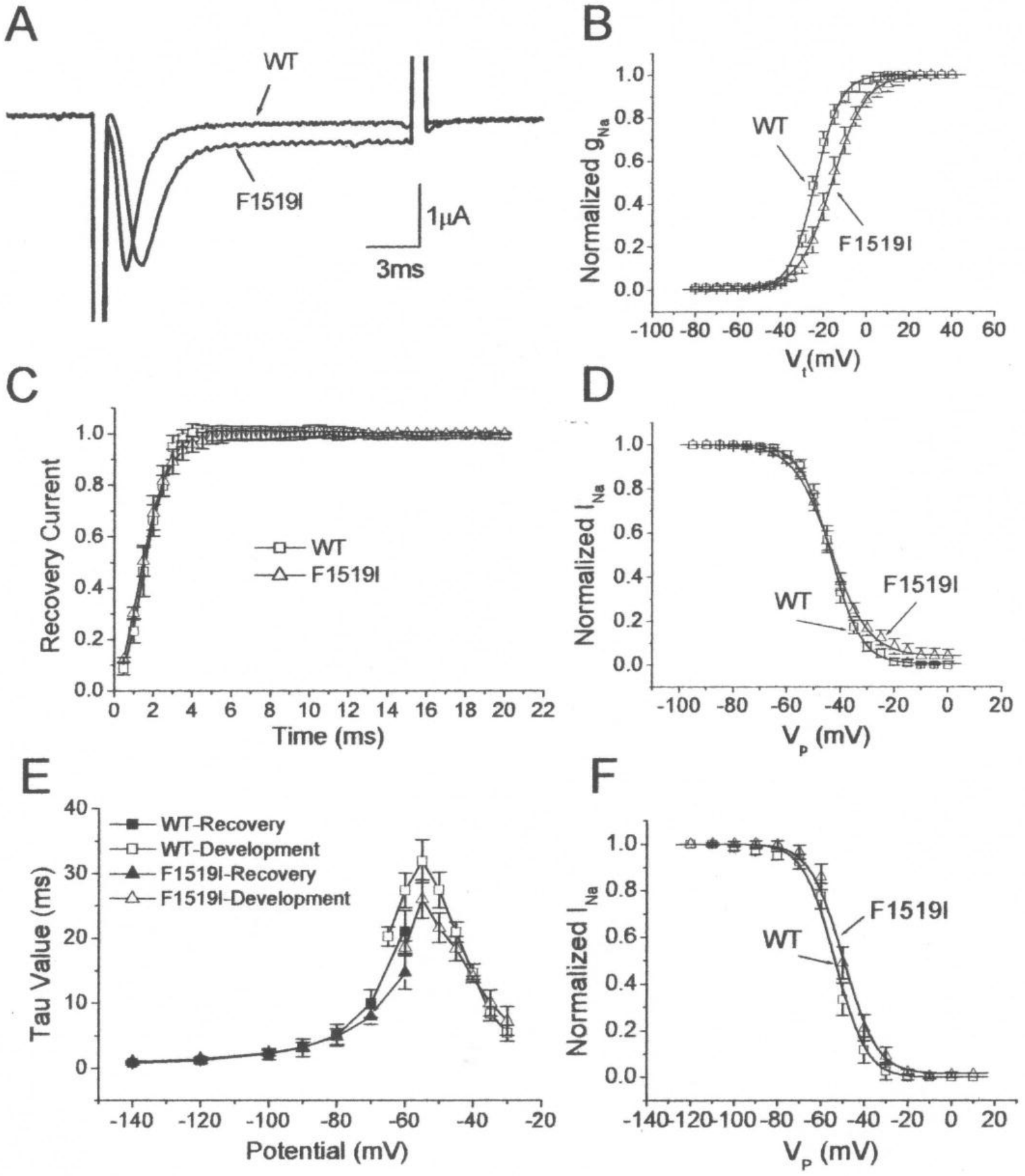
A
WT
F1519I
1μA
3ms
B
Normalized g_{Na}
WT
F1519I
V_t(mV)
C
Recovery Current
WT
F1519I
Time (ms)
D
Normalized I_{Na}
WT
F1519I
V_p (mV)
E
WT-Recovery
WT-Development
F1519I-Recovery
F1519I-Development
Tau Value (ms)
Potential (mV)
F
Normalized I_{Na}
WT
F1519I
V_p (mV)

Figure 3

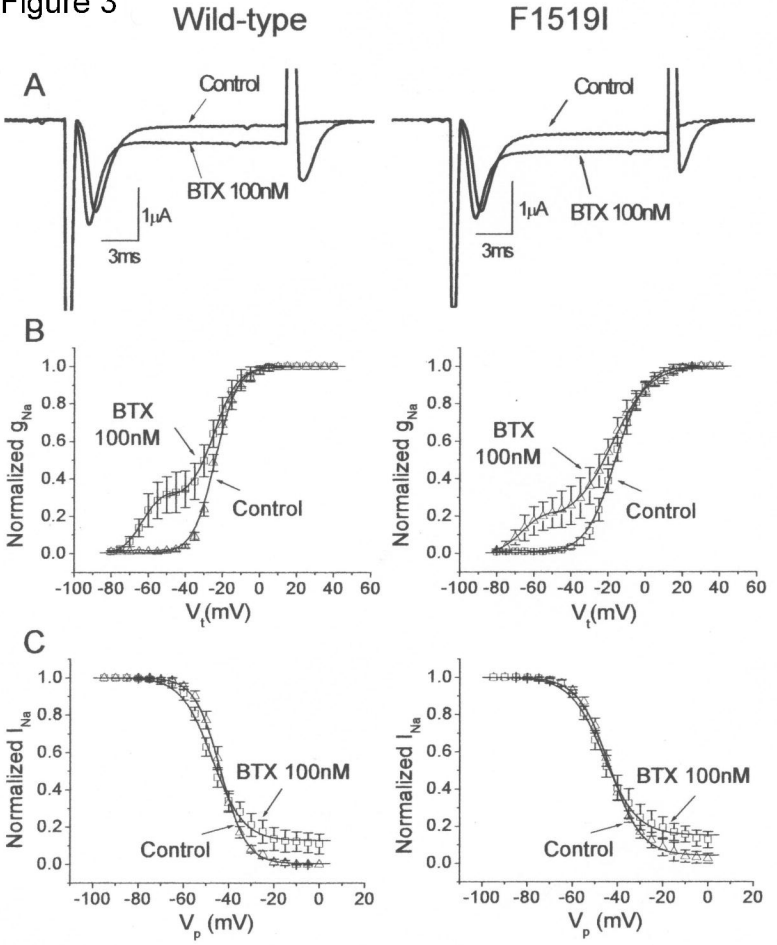
Wild-type
F1519I
A
Control
BTX 100nM
1μA
3ms
Control
BTX 100nM
1μA
3ms
B
Normalized g_{Na}
BTX 100nM
Control
V_t(mV)
Normalized g_{Na}
BTX 100nM
Control
V_t(mV)
C
Normalized I_{Na}
BTX 100nM
Control
V_p (mV)
Normalized I_{Na}
BTX 100nM
Control
V_p (mV)

Figure 4

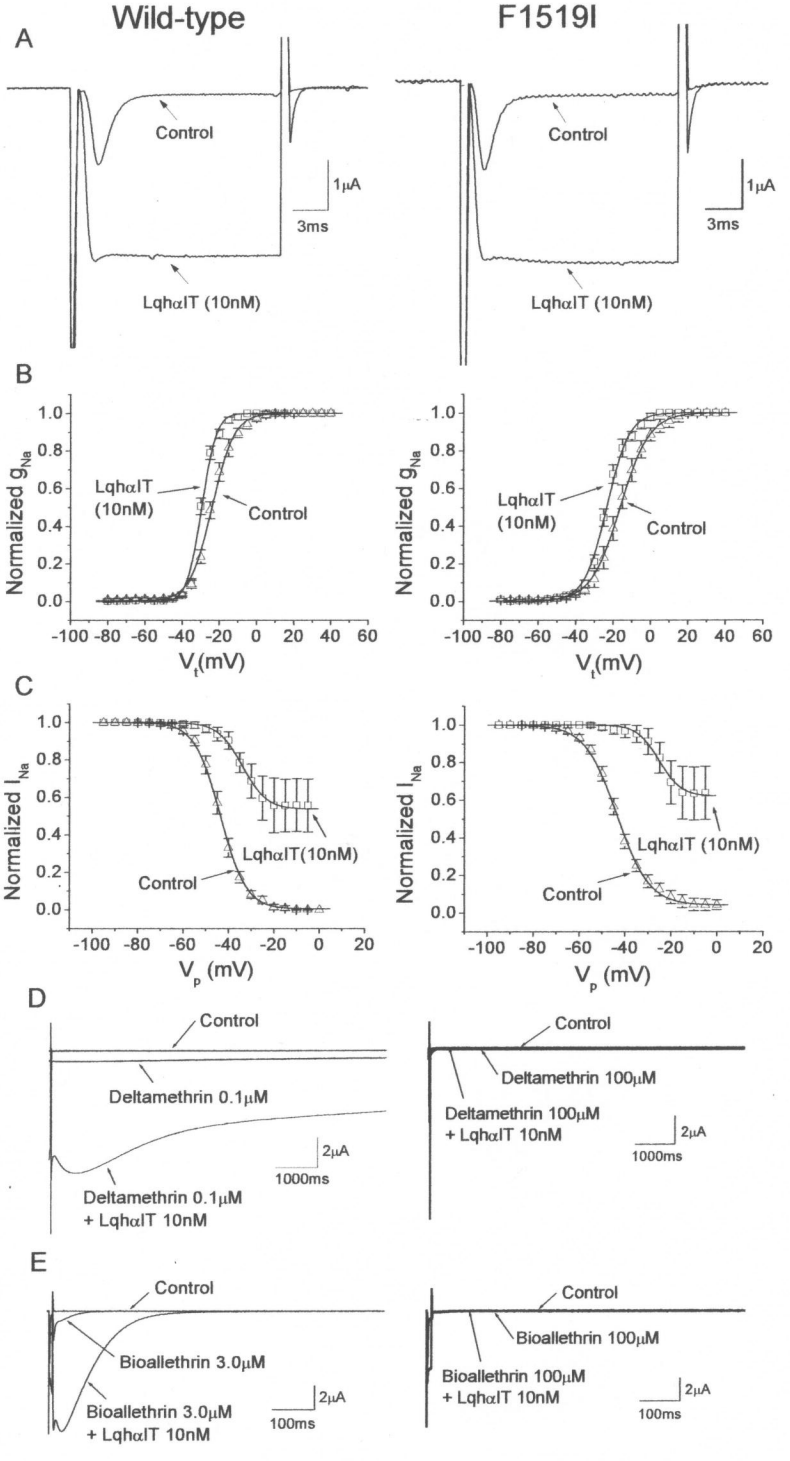
Wild-type
F1519I
A
Control
1μA
3ms
LqhαIT (10nM)
B
Normalized g_{Na}
LqhαIT (10nM)
Control
V_t(mV)
C
Normalized I_{Na}
LqhαIT(10nM)
V_p (mV)
D
Deltamethrin 0.1μM
2μA
1000ms
Deltamethrin 0.1μM + LqhαIT 10nM
Deltamethrin 100μM
Deltamethrin 100μM + LqhαIT 10nM
E
Bioallethrin 3.0μM
Bioallethrin 3.0μM + LqhαIT 10nM
100ms
Bioallethrin 100μM
Bioallethrin 100μM + LqhαIT 10nM

Figure 5

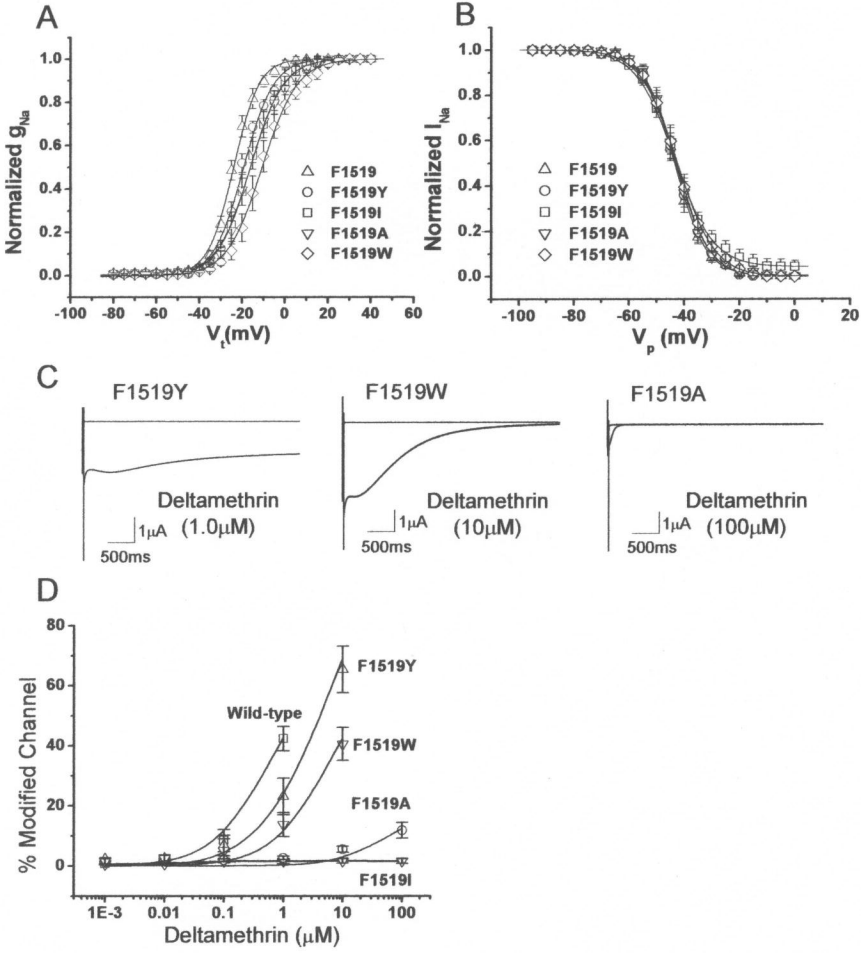
A
Normalized g_{Na}
1.0
0.8
0.6
0.4
0.2
0.0
-100 -80 -60 -40 -20 0 20 40 60
V_t(mV)
F1519
F1519Y
F1519I
F1519A
F1519W
B
Normalized I_{Na}
1.0
0.8
0.6
0.4
0.2
0.0
-100 -80 -60 -40 -20 0 20
V_p (mV)
F1519
F1519Y
F1519I
F1519A
F1519W
C
F1519Y
Deltamethrin
1μA (1.0μM)
500ms
F1519W
Deltamethrin
1μA (10μM)
500ms
F1519A
Deltamethrin
1μA (100μM)
500ms
D
% Modified Channel
80
60
40
20
0
Wild-type
F1519Y
F1519W
F1519A
F1519I
1E-3 0.01 0.1 1 10 100
Deltamethrin (μM)

Figure 6

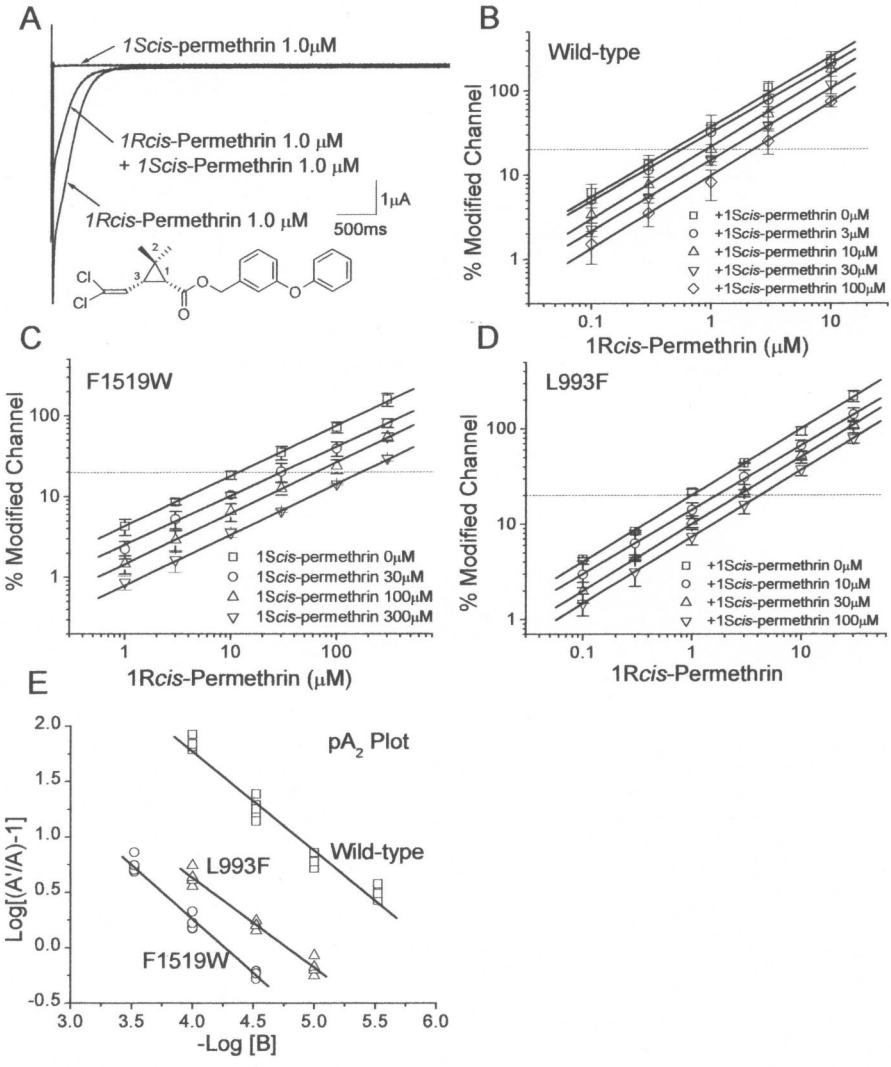
A
1Scis-permethrin 1.0μM
1Rcis-Permethrin 1.0 μM
+ 1Scis-Permethrin 1.0 μM
1Rcis-Permethrin 1.0 μM
1μA
500ms
Cl
Cl
O
O
B
Wild-type
% Modified Channel
+1Scis-permethrin 0μM
+1Scis-permethrin 3μM
+1Scis-permethrin 10μM
+1Scis-permethrin 30μM
+1Scis-permethrin 100μM
1Rcis-Permethrin (μM)
C
F1519W
% Modified Channel
1Scis-permethrin 0μM
1Scis-permethrin 30μM
1Scis-permethrin 100μM
1Scis-permethrin 300μM
1Rcis-Permethrin (μM)
D
L993F
% Modified Channel
+1Scis-permethrin 0μM
+1Scis-permethrin 10μM
+1Scis-permethrin 30μM
+1Scis-permethrin 100μM
1Rcis-Permethrin
E
pA2 Plot
Wild-type
L993F
F1519W
Log[(A'/A)-1]
-Log [B]

Molecular Pharmacology Fast Forward. Published on November 3, 2004 as DOI: 10.1124/mol.104.006205
This article has not been copyedited and formatted. The final version may differ from this version.

Figure 7